

1995120857

405736
6p.

High Performance Stepper Motors for Space Mechanisms

Patrick Segal* and Christine Estevenon*

Abstract

Hybrid stepper motors are very well adapted to high performance space mechanisms. They are very simple to operate and are often used for accurate positioning and for smooth rotations. In order to fulfill these requirements, the motor torque, its harmonic content, and the magnetic parasitic torque have to be properly designed. Only finite element computations can provide enough accuracy to determine the toothed structures' magnetic permeance, whose derivative function leads to the torque. It is then possible to design motors with a maximum torque capability or with the most reduced torque harmonic content (<3% of fundamental). These later motors are dedicated to applications where a microstep or a synchronous mode is selected for minimal dynamic disturbances. In every case, the capability to convert electrical power into torque is much higher than on DC brushless motors.

Hybrid stepper motors operation in space mechanisms

Hybrid stepper motors are brushless synchronous motors usually dedicated to open-loop applications. They naturally generate controlled movements in position and speed. The usual applications are mainly for deployment, orientation, accurate pointing or positioning mechanisms (e.g., solar panels, antennas, optical devices). They are also an answer to classic motorization problems, as at average speeds (a few hundred rpm) there is no need for an angular or speed sensor, or a complex electronic driver. These motors can either be used in direct drive mechanisms or associated with a gearbox.

Their specific characteristics are required in numerous high performances space mechanisms :

- High incremental resolution (i.e., 0.3° full step) enhanced by microstep command possibilities.
- Very high torque capability per power unit (Motor Constant in $\text{N}\cdot\text{m}/\sqrt{\text{W}}$) and per mass unit (I_m in $\text{N}\cdot\text{m}/\sqrt{\text{W}}/\text{kg}$).
- High angular stiffness thanks to the natural high number of poles (up to 300).
- Excellent positioning accuracy and stability on steps and microsteps.
- Possibility of open loop continuous rotation at very low speeds (down to 0.001 rpm) and with a good instantaneous stability. The type of command is then "synchronous," with sinusoidal phase currents.

Moreover, special efforts must be done when designing these motors, such as :

- Research for a minimal torque harmonic content for very smooth movements (displacements of large inertia or micro-gravity experiences).
- Minimization of the motor parasitic torques (magnetic friction and detent torque) for improved positioning performances.

* SAGEM, Paris, France

Hybrid stepper motors design

Hybrid stepper motors (Fig. 1) produce a torque, which has a general expression of:

$$T = \frac{N_R}{2} \sum_{i=1}^{2p} F_i^2 \frac{\partial P_i}{\partial \theta_e} \quad (1)$$

Where N_R : Number of rotor teeth.
 e : Electrical angle = $N_R \theta_m$.
 m : Mechanical angle.
 F_i : Magneto Motive Force under pole i .
 P_i : Air gap permeance under pole i .

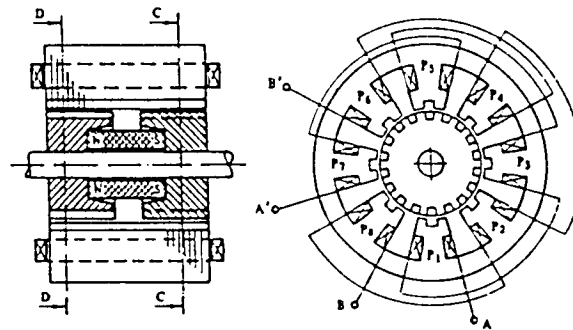


Figure 1 - Hybrid stepper motor

$P_i = P(\theta_m)$ is the permeance function. It characterizes the possibility offered to the magnetic field to go through the air gap more or less easily. This is done according to the relative position of the rotor and stator teeth: P_i is maximal for aligned teeth, minimal for misaligned teeth.

$P(\theta_m)$ is of period $\frac{2\pi}{N_R}$ and can be written as a Fourier series. The relation (1) sets the tight link between the torque and its harmonic content and the permeance harmonics (P_0, P_1, P_2, \dots).

This approach has been synthesized from the equivalent circuit diagram of a standard two-phase motor [1]. Simple analytical relations have been established between torque and permeance harmonics for a One-Phase-On mode. The same calculations for the synchronous mode ($F_i = F_0 \sin(\omega t - \frac{i\pi}{2})$) give a similar expression:

$$T = N_R \left[\begin{array}{l} -2 \frac{F_0 \varnothing_m P_1}{P_D} \sin(\theta_e - \omega t) + F_0^2 \left(\frac{2P_1^2}{P_D} - P_2 \right) \sin(2(\theta_e - \omega t)) - F_0^2 P_2 \sin(2(\theta_e + \omega t)) \\ -6 \frac{F_0 \varnothing_m P_3}{P_D} \sin(3\theta_e + \omega t) - 4P_4 \left(F_0^2 + \frac{2\varnothing_m^2}{P_D^2} \right) \sin(4\theta_e) - 10 \frac{F_0 \varnothing_m P_5}{P_D} \sin(5\theta_e - \omega t) \end{array} \right]$$

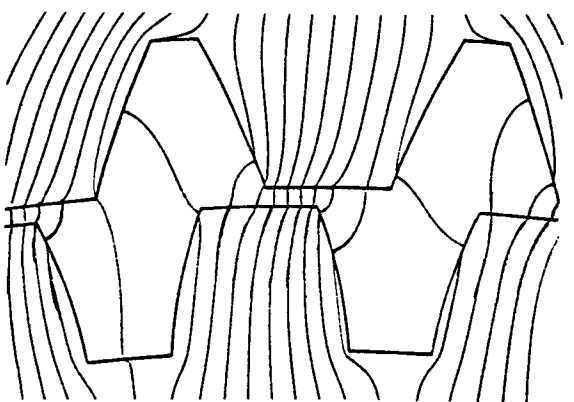
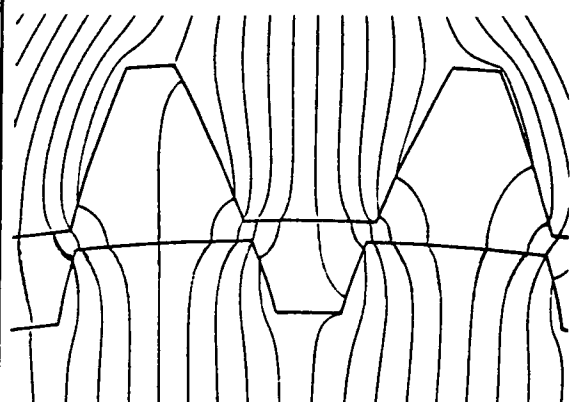
with: Φ_m : Magnet magnetic flux.
 P_D : $4P_o + P_m + P_r$
 P_m : Magnet permeance.
 P_r : Rotor leakage permeance.

The maximal motor torque implies a maximal ratio $\frac{P_1}{P_D}$. This ratio depends on the teeth geometry (P_o , P_1), on the magnet geometry (P_m), and on the rotor magnetic leakage (P_r). The torque harmonics are defined by the harmonic content of the air gap permeance. This one is completely defined by the teeth geometry, the teeth sizes compared to the air gap, and by the teeth magnetic saturation level.

Air gap permeance calculations

Simple analytical models have been proposed for the air gap permeance calculations [2]. Even though they can be improved mainly by taking into account the natural difference between rotor and stator tooth pitches, they are not accurate enough; the fundamental harmonic accuracy is not better than $\pm 10\%$ and the harmonic content they generate has nothing to do with the actual values.

Only finite element computations can give accurate values for $P(\theta_m)$, and will do so even if the teeth are highly saturated [3]. The toothed structures geometry optimization

Toothed structure A : High torque $N_R = 50$ - Airgap = 0.12 mm	Toothed structure B : Low torque harmonic content $N_R = 50$ - Airgap = 0.15 mm
 <p data-bbox="324 1587 609 1808"> $P_o = 4.241$ $P_1 = 0.839 = 100 \%$ $P_2 = 0.008 = 1.0 \%$ $P_3 = 0.021 = 2.5 \%$ $P_4 = 0.000 = 0.0 \%$ $P_5 = 0.000 = 0.0 \%$ </p>	 <p data-bbox="917 1587 1202 1808"> $P_o = 4.978$ $P_1 = 0.620 = 100 \%$ $P_2 = 0.004 = 0.6 \%$ $P_3 = 0.002 = 0.3 \%$ $P_4 = 0.000 = 0.0 \%$ $P_5 = 0.000 = 0.0 \%$ </p>

is then possible according to different design purposes. (See the table with air gap permeances in 10^{-5} H/m . The stator is the same in the two cases.)

Parasitic torque

The parasitic torque is defined as the torque required to rotate the unpowered motor at low speed. This characteristic can be important when two motors are integrated on the same axis for total redundancy. This parasitic torque includes :

- The very well-known detent torque, written according to [1] or relation (2) with $F_o = 0$:

$$T_d = - 8P_4 \frac{\varnothing_m^2}{P_D^2} \sin(4\theta_e)$$

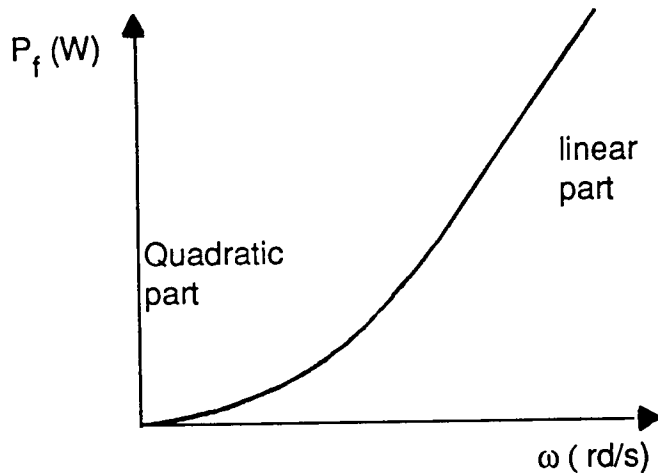
This fourth harmonic torque depends on the fourth harmonic permeance (P_4) and on the square value of the permanent magnet magnetic flux (\varnothing_m^2). These two parameters are defined when designing the motor.

- A torque related to the hysteresis phenomena inside the magnetic circuit which includes two components:
 - A "dry friction" component, $T_f = - \text{Sign}(\dot{\theta}) \cdot T_f$, which does not depend on the rotor angular position.
 - A component coming from the magnetic remanence effects in the toothed structures, especially when they are highly saturated, given as:

$$T_p = - T_p \sin(\theta_e + \gamma)$$
 γ is a phase shift with the torque created just before the currents have been switched off. T_p and γ depend on the "magnetic history" of the motor magnetic circuit which is linked to:
 - The magnetic materials characteristics (B(H) cycles, permanent magnet type).
 - The phase current relation versus time.
 - The rotor dynamic position ($\theta, \dot{\theta}$).

Modelling and evaluation of T_f and T_p are quite difficult to establish [4]. Materials with thin B(H) cycles and low levels of magnetic induction will contribute to lower their amplitudes. They will also lower the torque capabilities per mass unit.

Finally, at higher rotation speeds, the well-known iron losses have to be taken into account. Their experimental shape is the following:



Results

SAGEM has designed a complete range of stepper motors for various space mechanisms. Their holding torques are from 0.2 N•m up to 6.0 N•m for an electrical power between 2 W and 10 W. The numbers of steps are the standard 200 steps/revolution and also 360 and 1200 steps/revolution for high-resolution applications. The SAGEM stepper motors are generally proposed in a frameless configuration for an optimized mechanical integration inside the mechanisms. An annular shape is offered for large outside diameter motors. Magnetic and mechanical modular designs have been selected. It's now possible to create new motors, with different lengths, from a basic magnetic structure. Housed configurations with bearings are also available, as well as redundant windings.

The most important electromechanical performances are presented in Figure 2. They have been measured on motors designed for:

- High torque (Application A)
- Low torque or speed harmonic content (Application B).

The first motors (A) have:

- A very high capability to convert the electrical power into static torque per mass unit: I_m can reach 0.6 to 0.8 N•m/ \sqrt{W} /kg. It is between 3 and 6 times higher than the best DC brushless motors characteristics.
- A positioning accuracy better than 3% of the step angle (Peak to Peak) in the following conditions: step to step mode, no load conditions, back and forth rotation. Positioning repeatability and stability are one order of magnitude lower, around 0.5% of the step angle under similar dynamic approach conditions.

The second motors (B) offer:

- Lower torque capability per mass unit (-15% to -20% for I_m).
- A very low torque harmonic content (<3% of the fundamental), roughly without 3rd and 4th harmonics (<1% each).
- A low speed harmonic content in synchronous mode (<15% of the nominal constant speed). The fourth speed harmonic is the most important one (between 5% and 8%). It can be canceled by adding a third harmonic component in the phase currents according to well-known techniques.

Acknowledgments

This work has been funded by a R&D/CNES contract (1992/1994). The authors wish to thank Mr. Borrien and his team for their support.

References

1. Kuo, B. C. Torque components of hybrid PM step motors - Incremental Motion Control Systems and Devices. 1984.
2. Kuo, B. C. Permeance models and their applications to step motor design - Incremental Motion Control Systems and Devices. 1986.
3. Huard, S. R. and C. K. Taft. A finite element lumped parameter model for 1.8° stepping motors - Incremental Motion Control Systems and Devices. 1990.
4. Jufer, M. Hysteresis effect on the hybrid step motor statical and dynamical behaviour - Incremental Motion Control Systems and Devices. 1989.

Figure 2. Performance of some SAGEM Stepper Motors

	References						
	21PP61	23PP43	23PP63	35PP81	57PP41	57PP81	57PP82
Number of steps/rev. (step angle)	200 (1.8°)	200 (1.8°)	200 (1.8°)	360 (1°)	1200 (0.3°)	1200 (0.3°)	1200 (0.3°)
Basic application	A	B	A	A	B	A	A
Outside Diameter (mm) *	53	59	59	88	155	155	155
Inside Diameter (mm) *	10	10	10	55	94	94	94
Length (mm) *	22	40	40	25	30	30	44
Total mass (g) *	180	525	525	320	1400	1400	2400
Holding torque (Nm) **	0,16	0,34	0,40	0,60	2,4	3,0	5,5
Power (W)	2,0	1,4	1,4	5,2	8,2	8,2	10,0
Angular stiffness (Nm/rad)	8	17	20	54	720	900	1650
Total parasitic torque (Nm)	< 0,012	< 0,015	< 0,030	< 0,040	< 0,060	< 0,10	< 0,20
Detent torque (Nm)	< 0,004	< 0,003	< 0,010	< 0,015	< 0,005	< 0,01	< 0,01
Sum of the first ten torque harmonics (% of fundamental)		< 3 %			< 3 %		
Electromechanical ratios :							
Nm / kg	0,84	0,63	0,93	1,87	1,75	2,15	2,30
Nm / \sqrt{W}	0,11	0,29	0,34	0,26	0,84	1,05	1,74
Nm / \sqrt{W} / kg	0,63	0,55	0,64	0,82	0,60	0,75	0,72
Open loop performances :							
No load positioning accuracy (deg. max. Peak to Peak)	0,05°		0,03°	0,03°		0,02°	0,01°
Low synchronous speed (rpm)		0,01 to 1			0,001 to 1		
Sum of the first ten speed harmonics (% of fundamental)		< 15 %			< 15 %		

* In frameless configuration

** Without magnetic saturation effects